Original Research Article

Evaluation of Solar Cell Using Terahertz Time-Domain Spectroscopy

.

ABSTRACT

Terahertz time-domain spectroscopy (THz-TDS) has been used to investigate the optical properties of mono silicon solar cell. The sample was optically excited using continuous-wave (CW) light of wavelengths of 800 nm and 365 nm, and the carrier density and mobility were extracted from the THz-TDS data by fitting with the simple Drude model. The conductivity shows nonlinear increase with the optical excitation power. The mobility of the photo-excited carriers also increases nonlinearly with the CW light power. However, the mobility shows tendency to saturate with the increase of illumination power, which can be explained by carrier trapping effect to the impurity states existing in the band-gap region of the base material of solar cell. In addition, it is observed that the carrier density and mobility are smaller for 365 nm light illumination due to surface recombination.

Keywords: Terahertz spectroscopy, Solar cell, CW laser illumination.

1. INTRODUCTION

Solar energy is the most promising readily available source of energy. It is often mentioned as a part of the solution to the energy problems. However, increasing the energy conversion efficiency and reducing the cost of production are the major challenges to make solar electricity more competitive with the conventional energy sources [1, 2]. Today most of the solar cells are made of crystalline silicon because of its large abundance on the earth, low cost and high efficiency. The dynamic properties of photo-excited carriers also play an important role on the photovoltaic conversion efficiency of solar cell. Thus, it is important to understand the optical response of photo-excited carriers in solar cell to further improve the cell efficiency. A variety of measurement techniques for the characterization of photovoltaic cells, such as electroluminescence [3], light beam induced current [4] or voltage and current measurements, require electric contacts and can only be performed on the finished photovoltaic cells. On the other hand, a noncontact and nondestructive technique using terahertz (THz) waves is widely utilized on various materials such as semiconductors, liquids and superconductors to obtain a variety of physical properties [5-7]. The benefit of THz technique is that it can be used for the characterization of solar material or semi-finished solar cells without electric contacts at the beginning as well as during the production process of photovoltaic cells. By employing this technique, a wide variety of research, such as spectroscopic [8], imaging [9] and terahertz emission [10] have been done on investigation of solar cells and related materials. It was effectively applied to study the properties of irradiated silicon wafer for space solar cell application [8]. In our previous study, we used a laser terahertz emission microscope technique to study THz emission from a silicon solar cell and visualize the temporal photo-current generated by femtosecond laser pulse illumination [10]. We also used this technique to examine both the effects of optically generated carriers by a continuous-wave (CW) light illumination and applied bias voltage on the behavior of a solar cell [11]. Another advantage of THz spectroscopy is that the frequency dependent absorption coefficient and refractive index can be obtained from the detected signal. From this the complex dielectric constant and complex conductivity can be determined. After analyzing the conductivity data, we can easily get the carrier transport properties of material, e.g. charge carrier density and mobility. Under illumination, these two parameters are particularly important because they dominate the electrical behavior of solar cell. In this work, we applied transmission-type terahertz time-domain spectroscopy (THz-TDS) to investigate the optical properties and charge carrier dynamics in mono Si solar cell under CW light illumination. In particular, we measured illumination dependence of conductivity, charge carrier density and mobility.

2. EXPERIMENTAL DETAILS

The sample used in this study was a commercial mono silicon solar cell (cell without electrodes and antireflection coating) which is configured as a large-area *p–n* junction. Typical doping densities are 1×10^{19} cm^{-3} in n-type region and 1×10^{16} cm^{-3} in p-type region and the thickness of the emitter (n-type region) is ~0.5 μm [12]. The overall thickness of the sample was 182 μm measured by THz peak delay technique [13]. The schematic structure of the solar cell and its AFM images are shown in Fig. 1(a)-1(c). The front surface image in Figure 1(b) showed that the several pyramidal structures with different sizes are randomly distributed over the entire surface. These shapes play an important role in improving light coupling into solar cells. The root mean square (rms) average roughness value was 150 nm. On the other hand the rear surface is an unpolished rough surface as shown in Figure 1(c). The rms average roughness value was 240 nm, which is higher than that of front surface. The experimental setup used for THz-TDS measurement is also shown schematically in Figure 1(d). A femtosecond (fs) laser with the center wavelength of 780 nm is used for the excitation of low-temperature-grown GaAs (LT-GaAs) photoconductive antennas which are used for generation and detection of THz pulses. The terahertz radiation was focused onto the sample with a spot diameter of about 5 mm. The sample was illuminated with CW light with wavelengths of 800 nm and 365 nm with area of 0.5 cm^2 and 0.88 cm^2, respectively. The illumination area is larger than that of terahertz beam spot to ensure uniform illumination. Measurements were carried out on both surfaces of the sample at various illumination powers. All measurements were performed at room temperature with relative humidity of around 30-35%.

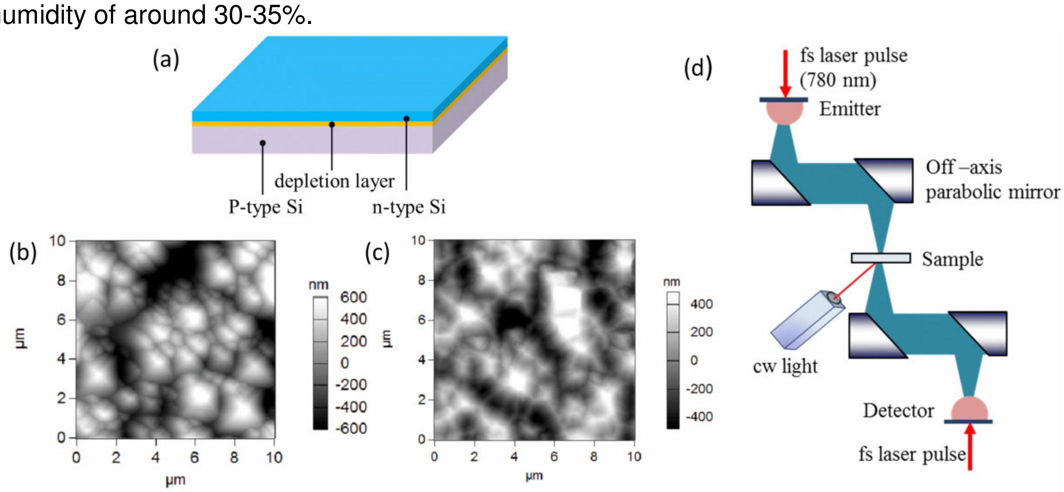

Fig. 1. (a) Schematic structure of mono Si solar cell and its AFM images of (b) front textured surface (c) rear rough surface. 1(d) Schematic of experimental setup for transmission-type THz-TDS

3. RESULTS AND DISCUSSION

Figure 2 (a) shows the waveforms of the THz pulses through the free space and the mono Si solar cell without CW light excitation. After applying Fast Fourier transform to the time domain spectra, the complex refraction index can be estimated. The complex refractive index with real part n and imaginary part κ (extinction coefficient) in the THz frequency region is shown in Fig 2(b). The real part of the refractive index is related to the speed of light in the medium, the imaginary part is directly related to the absorption of light through the material. The average value of refractive index of mono Si solar cell without light excitation is obtained as 3.39, which is very close to the reported value of 3.41 for crystalline silicon [6].

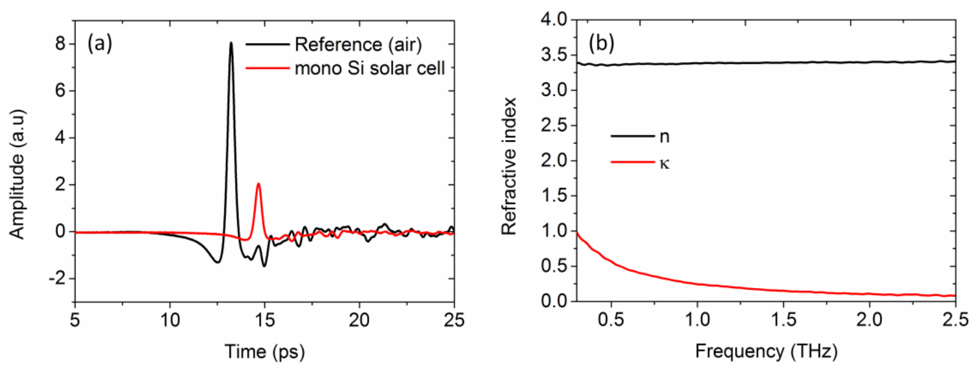

Fig. 2.(a) Waveforms of the terahertz pulses of free space and the pulses through mono Si solar cell. (b) Complex refractive index with real part n and imaginary part κof the cell

Figure 3(a) shows the waveforms of the THz pulses transmitted through the solar cell with illumination of the 800 nm CW laser from front surface at various powers. It is seen that the amplitude of the terahertz waveforms transmitting through the photo-excited sample is greatly reduced by the absorption of photo-excited carriers. By using the ratio between reference and sample waveforms in Fresnel coefficient equations, the transmission can be estimated. The transmittance of the THz wave at various illumination powers is presented in Fig. 3(b). The terahertz transmission decreases with the illumination power of CW laser due to increase of photo-excited carriers in the sample.

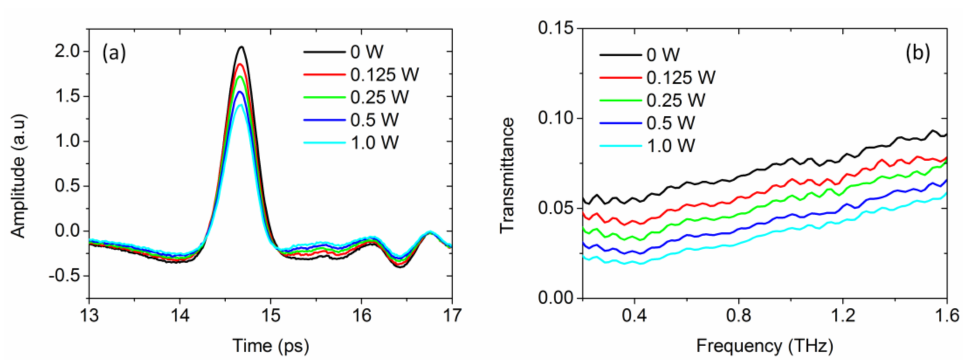

Fig. 3. (a) Waveforms of the THz pulses transmitted through the excited Si solar cell at 800 nm with various illumination powers. (b) Transmittance obtained from the waveforms in (a)

The complex conductivity is also obtained from the complex refractive index using $\tilde{n}^2 = \tilde{\varepsilon}(\omega) = \varepsilon_{Si} + i\tilde{\sigma}(\omega)/\omega\varepsilon_0$, where $\tilde{\varepsilon}$ is the complex dielectric constant, ε_0 is the permittivity of free space and ε_{Si} is the dielectric constant of undoped silicon [14]. Figure 4 shows frequency dependence of experimental data and the calculation of real part of conductivity of the solar cell with front illumination at 800 nm with various powers. The real part of the conductivity decreases with increasing frequency in the THz range. It is also evident that the conductivity increases with the illumination power of CW laser. The frequency dependence of the conductivity can be well described with the simple Drude model [15]. According to the Drude model, the complex conductivity is expressed as

$$\tilde{\sigma}(\omega) = \frac{\sigma_{dc}}{1 - i\omega\tau}$$

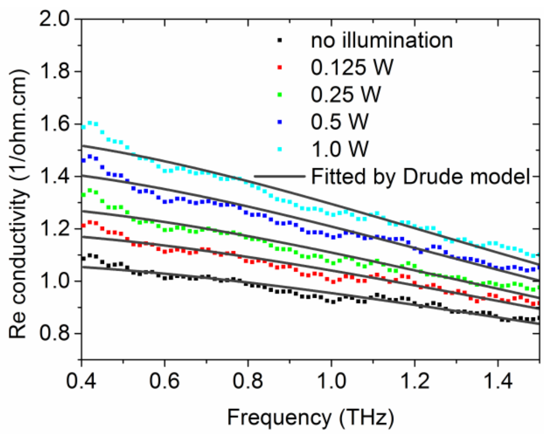

Fig. 4. Real part of conductivity of mono Si solar cell at 800 nm with various illumination powers from front surface; the solid lines are fitted curves with simple Drude model

whereσ_{dc} is the DC conductivity, τ is the average carrier scattering time. Solid lines in figure 4 are fitting lines to the real part of conductivity at each level of illumination power using the simple Drude model. The fitting parameters DC conductivity σ_{dc} and carrier scattering time τ are extracted from the fitted curves and presented in Table 1. The carrier density $N = \sigma_{dc} m^*/e^2\tau$ and the mobility $\mu = e\tau/m^*$are calculated by using the fitting parameters ofσ_{dc} and $\tau$with the effective mass $m^* = 0.26m_0$ for silicon [15].

Table 1.Fitting parameters based on simple Drude model under various illumination powers. The columns present the values for illumination power (*mW*), the DC conductivity $\boldsymbol{\sigma_{dc}}$ (1/Ω cm) and the carrier scattering time $\boldsymbol{\tau}$ (ps) extracted from the fitted curves; the excess carrier density *N* (cm^{-3}) and the mobility $\boldsymbol{\mu}$ (cm^2/Vs) determined by $\boldsymbol{\sigma_{dc}}$and $\boldsymbol{\tau}$.

800 nm					*365 nm*				
Power	σ_{dc}	τ	*N*	μ	*Power*	σ_{dc}	τ	*N*	μ
125	1.20	0.0618	4.0×10^{14}	417	100	1.096	0.0579	2.0×10^{14}	392
250	1.30	0.0665	6.0×10^{14}	449	200	1.107	0.0588	1.0×10^{14}	398
500	1.45	0.0708	1.4×10^{15}	478	300	1.113	0.0575	5.0×10^{14}	389

1000	1.57	0.0732	$2.3x10^{15}$	495	400	1.118	0.0598	$-3.0x10^{14}$	404

The DC conductivity, excess carrier density and mobility are plotted in Figure 5 as a function of the illumination power. It is shown in Fig. 5(a) that the DC conductivity rises nonlinearly with the illumination power of CW laser and tends to saturate with the increase of illumination power. It is also found in Fig. 5(b) that the excess carrier density increases linearly and, the mobility increases and tends to saturate with the illumination power of CW laser. This tendency to saturate in mobility may be explained by the saturation effect of photo-excited carrier trapping in the impurity states in the band-gap of the solar cell [16-20]. Minority carrier traps are often present in the solar grade crystalline silicon [18, 19]. Due to laser illumination, electron-hole pairs are generated in the base (p-type) of the solar cell. A part of minority electrons would be captured or scattered by impurity states which temporarily hold electrons. As the illumination power increases, these states progressively trap electrons and become neutral. Therefore, the capture and scattering cross sections for electronsare reduced significantly with increasing excess carrier density, which increases the mobility of minority carriers.

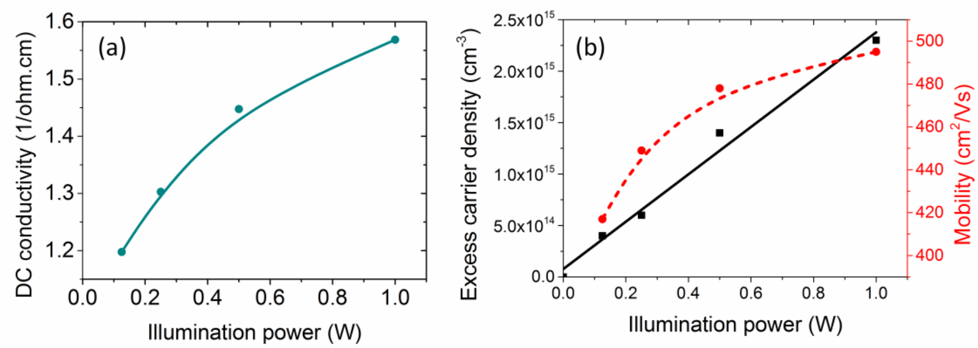

Fig. 5. 800 nm laser Illumination power dependence of (a) DC conductivity and (b) excess carrier density and mobility deduced from the simple Drude model fitted to the real conductivity

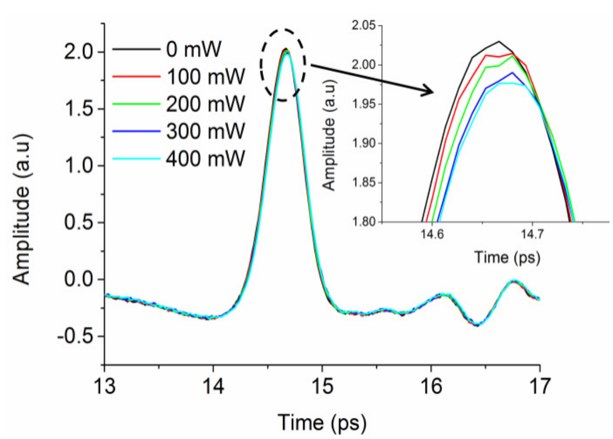

Fig. 6. Waveforms of the THz pulses transmitted through the excited Si solar cell at 365 nm with various illumination powers

We also carried out similar measurements under 365nm light illumination. Figure 6 shows the waveforms of the THz pulses transmitted through the solar cell with illumination of the

365 nm light at various powers. The amplitude of the THz waveforms decreases very small with the illumination power. After analyzing the waveforms data, the excess carrier density and mobility are calculatedand also presented in Table 1. The excess carrier density is smaller for illumination at 365 nm than that for 800 nm. This can be explained by considering the penetration depth of 365 nm light. The penetration depth in silicon for 365 nm is about 0.01 µm [21]. Under 365 nm light illumination, the photo-excited carriers are generated within 10 nm from the surface of the solar cell and their lifetime strongly affected by the high surface recombination.

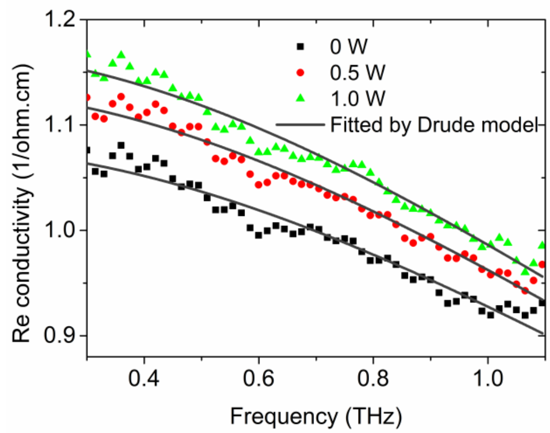

Fig. 7. Real part of conductivity of mono Si solar cell at 800 nm with various illumination powers from rear surface; the solid lines are fitted curves with simple Drude model

More measurements also performed with illumination at 800 nm from rear surface of the solar cell. In these measurements the THz pulse are transmitted from the back surface to the front surface of the solar cell. Figure 7 shows the real part of conductivity data fitted with the simple Drude model. From the fitting parameters the excess carrier density and mobility are calculated. The calculated excess carrier densities are $1x10^{14}$ and $2x10^{14}$ cm^{-3} and the mobility are 455 and 466 cm^2/Vs for 0.5 and 1.0 W illumination, respectively. From these results it is seen that the carrier density and mobility increase with increasing illumination power, which are similar to the front illumination results. However, the value of carrier density and mobility are smaller than those of the front illumination results. For example, at 1 watt illumination the carrier density and mobility are decreased by 21% and 5.9%, respectively, compared to the front illumination results. This is because the reflectance of rear surface is much larger than that of textured front surface [22]. Textured front surface reduces the reflection of CW laser and generated more photo carriers. Moreover, the unpolished rear surface recombination is thought to be higher than that of the front surface because it contains a large number of defects and impurities that act as a recombination centers.

4. CONCLUSION

We have employed transmission-type THz-TDS system to measure optical properties of mono Si solar cell during photo-excitation by 800nm and 365nm CW light. The terahertz transmission is greatly reduced by the absorption of photo-excited carriers generated by the 800nm CW laser illumination. The analysis of transmission data yields complex refractive index as well as conductivity. The conductivity data can be fitted with the simple Drude model and from the fitting results the excess carrier density and mobility are deduced. The carrier mobility increases and saturated with the illumination of CW laser. This phenomenon is explained by the effect of carrier trapping in the impurity states in the band gap of solar cell. We also observed small effect under 365nm light illumination due to the high surface recombination.

REFERENCES

1. Choubey PC, Oudhia A and Dewangan R. A review: Solar cell current scenario and future trends. Recent Research in Science and Technology. 2012;4(8):99-101.
2. Saga Tatsuo. Advances in crystalline silicon solar cell technology for industrial mass production.NPG Asia Mater. 2010;2(3):96-102.
3. Fuyuki T and Kitiyanan. Photographic diagnosis of crystalline silicon solar cells utilizing electroluminescence.ApplPhys A. 2009;96:189-196.
4. Thantsha NM, Macabebe EQB, Vorster FJ, Van Dyk EE, Opto-electronic analysis of silicon solar cells by LBIC investigations and current-voltage characterization. Physica B. 2009;404:4445-4448.
5. Tonouchi M. Cutting-edge terahertz technology. Nat. Photonics. 2007;1(2):97–105.
6.Grischkowsky D, Keiding S, Exter M, and Fattinger C. Far-infrared time-domain spectroscopy with terahertz beams of dielectrics and semiconductors. J. Opt. Soc. Am. B. 1990;7(10):2006-2015.
7. Pedersen JE and Keiding SR. THz time-domain spectroscopy of nonpolar liquids.IEEE J. Quantum Electronics. 1992;28:2518-2522.
8. Nagai N, Sumitomo M, Imaizumi M, and Fukasawa R. Characterization of electron- or proton-irradiation Si space solar cells by THz spectroscopy. Semicond. Sci. Technol. 2006;21:201-209.
9. Minkevičius L et al. Solar cell imaging and characterization by terahertz techniques. Proc. SPIE. 2012;8496:8496131-6.
10. Nakanishi H, Fujiwara S, Takayama K, Kawayama I, Murakami H, Tonouchi M. Imaging of a polycrystalline silicon solar cell using a laser terahertz emission microscope. Appl. Phys. Express. 2012;5:112301.
11. Salek KA, Nakanishi H, Ito A, Kawayama I, Murakami H, Tonouchi M. Laser terahertz emission microscopy studies of a polysilicon solar cell under the illumination of continuous laser light. Optical Engineering. 2014;53(3):0312041-6.
12. Nelson J. The Physics of Solar Cells, Imperial College Press, London; 2003.
13. Jen C and Richter C. Sample thickness measurement with THz-TDS: Resolution and Implications. J Infrared MilliTerahz Waves. 2014;35:840–859.
14. Sakai K (Ed.). Terahertz Optoelectronics.Springer; 2005.
15. Exter M and Grischkowsky D. Carrier dynamics of electrons and holes in moderately doped silicon. Phys. Rev. B. 1990;4:12140-12149.
16. Fabre E, Mautref M and Mircea A. Trap saturation in silicon solar cells. Applied Physics Letters. 1975;27(4):239-241.
17. Fan HY. Effect of traps on carrier injection in semiconductors.Physical review. 1953;92 (6)1424-1428.
18. Macdonald D and Cuevas A. Trapping of minority carriers in multicrystalline silicon. Appl. Phys. Lett. 1999;74(12):1710-1712.
19. Schmidt J and Cuevas A. Electronic properties of light-induced recombination centers in boron-doped Czochralski silicon. J. Appl. Phys. 1999;86(6):3175-3180.
20. Macdonald D, Kerr M and Cuevas A. Boron-related minority-carrier trapping centers in p-type silicon. Appl. Phys. Lett. 1999;75(11):1571-1573.
21. Aspnes DE and Studna AA. Dielectric functions and optical parameters of Si, Ge, GaP, GaAs, GaSb, InP, InAs, and InSb from 1.5 to 6.0 eV. Phys. Rev. B. 1983;27:985-1009.

22. Barrio R, Gonzalez N, Carabe J and Gandia JJ. Optimisation of NaOHtexturisation process of silicon wafers for heterojunction solar-cells applications. Solar energy. 2012;86:845-854.